JOURNAL OF GEOPHYSICAL RESEARCH VOL. 69, NO. 3 FEBRUARY 1, 1964

Analysis of Topside Sounder Records

R. J. FITZENREITER AND L. J. BLUMLE

Goddard Space Flight Center, Greenbelt, Maryland

Abstract. A large number of features can be seen on the ionograms obtained by the Canadian topside sounder satellite. The most useful feature for the calculation of electron density profile is the extraordinary trace; however, to achieve accurate results, the effect of the geomagnetic field must be carefully considered in the data reduction process. The method of analysis we selected assumes that small sections of the profile can be approximated by exponential laminations. This method requires fewer points than other first-order lamination techniques to achieve a given accuracy. It is usually assumed in the analysis that the received echoes correspond to vertical propagation. This assumption is not always valid, and it can in some cases lead to large errors. The sounder also excites the medium in the immediate vicinity of the satellite, giving rise to various plasma resonances. A graph is given which summarizes the local effects that are seen on the ionograms. This graph can be used for a rapid identification of these resonances.

Introduction. The success of the first topside sounder satellite, Alouette, launched on September 29, 1962, has provided a new means of studying the electron density distribution in the upper ionosphere [*Warren*, 1962; *Petrie*, 1963; *Lockwood*, 1963; *Nelms*, 1963; *Muldrew*, 1963*a*; *Hagg*, 1963]. The principal equipment on Alouette is the ionospheric sounder, which sweeps from 0.5 to 11.5 Mc/s while the satellite moves about 80 km along its 1000-km circular, 80° inclination orbit; this sweep is repeated every 125 km along the orbital path. The sweep and orbital characteristics provide approximately one ionogram per degree of latitude for all except high latitudes. The orbital precession of nearly −8 min in time per day is such that, by combining southbound and northbound passes, we can obtain data at all local mean times every three months.

It is the purpose of this paper to discuss the interpretation of the data and to outline a technique for reducing Alouette data to electron density distributions with height.

Characteristics of topside ionograms. Illustrated in Figure 1 are two examples of typical Alouette ionograms observed at midlatitudes and the corresponding N–h profiles. These ionograms differ from the conventional bottomside ionograms in that the virtual depth p', derived using the free-space wave velocity, is measured down from the satellite. The ordinary, extraordinary, and z-mode echoes are identified along with the plasma resonances and ground echoes.

The plasma resonances, first discussed by *Lockwood* [1963], occur at the electron gyrofrequency and its harmonics and at frequencies where the phase refractive index is infinite or zero at the satellite. One additional phenomenon which is similar in appearance to a plasma resonance occurs on the ionograms when the refractive index is infinite for the vertical ray. The conditions for all these phenomena are given by the following formulas.

$f_N^2 = f^2$	$X = 1$	$= f_N^2/f^2$
$f_N^2 = f^2 + ff_H$	$X = 1 + Y$	$= 1 + (f_H/f)$
$f_N^2 = f^2 - ff_H$	$X = 1 - Y$	$= 1 - (f_H/f)$
$f_N^2 = f^2 - f_H^2$	$X = 1 - Y^2$	$= 1 - (f_H^2/f^2)$
$f_N^2 = \dfrac{f^2 - f_H^2}{1 - (f_H^2 \cos^2\theta/f^2)}$	$X = \dfrac{1 - Y^2}{1 - Y_L^2}$	$= \dfrac{1 - (f_H^2/f^2)}{1 - (f_H^2 \cos^2\theta/f^2)}$

where

f = wave frequency.
f_N = electron plasma frequency.
f_H = electron gyrofrequency.

θ = angle between the wave normal and the magnetic field.

The reflection conditions for the ordinary, z, and extraordinary modes (f_o, f_z, and f_x) are:

$$f_0 = 10^{-3}\sqrt{80.6N}$$

$$f_z = 0.5\left(-f_H + \sqrt{f_0^2 + \frac{f_H^2}{4}}\right)$$

$$f_x = 0.5\left(f_H + \sqrt{f_0^2 + \frac{f_H^2}{4}}\right)$$

where N is the electron density per cubic centimeter, and all frequencies are in megacycles per second. These 'resonance' conditions are represented graphically in Figure 2, where the abscissa is the plasma frequency f_N, normalized with respect to the electron gyrofrequency f_H, and the ordinate is the normalized wave frequency f/f_H. With a graph of this type, the identification of resonances can be rapidly verified. The zeros of the refractive index are represented for the ordinary, extraordinary, and z mode by the lines labeled $X = 1$, $X = 1 - Y$, and $X = 1 + Y$, respectively. The pole of the refractive index for the vertical ray occurs at $X = (1 - Y^2)/(1 - Y_L^2)$ and is illustrated (for $Y_L = Y \cos 45°$) by the dashed line. This condition can occur in the region bounded by the curves $X = 1$, $Y = 1$, and $X = 1 - Y^2$. At the magnetic equator it will coincide with the line $X = 1 - Y^2$, whereas at the magnetic dip pole it will occur along the $Y = 1$ line if the normalized plasma frequency is less than unity and will coincide with the ordinary plasma resonance ($X = 1$) for normalized plasma frequencies greater than unity. The line $X = 1 - Y^2$ represents the limit of z-mode propagation, and at this point the refractive index is infinite in the plane perpendicular to the magnetic field. The z mode can therefore only propagate in the region bounded by the curves $X = 1 + Y$ and $X = 1 - Y^2$, and the ordinary and extraordinary modes can propagate only in the regions above the curves $X = 1$ and $X = 1 - Y$, respectively.

The plasma resonances observed at the electron gyrofrequency and its first two harmonics are represented by the dotted lines labeled $Y = 1$, 1/2, 1/3. Others have shown that the $X = 1$, $1 - Y^2$, correspond to well-known plasma oscillations.

For a fixed electron density the propagation conditions encountered as the sounder sweeps from 0.5 to 11.5 Mc/s are represented by the vertical line AI on Figure 2. As the sounder sweeps up in frequency the normalized wave frequency increases, but no propagation can take

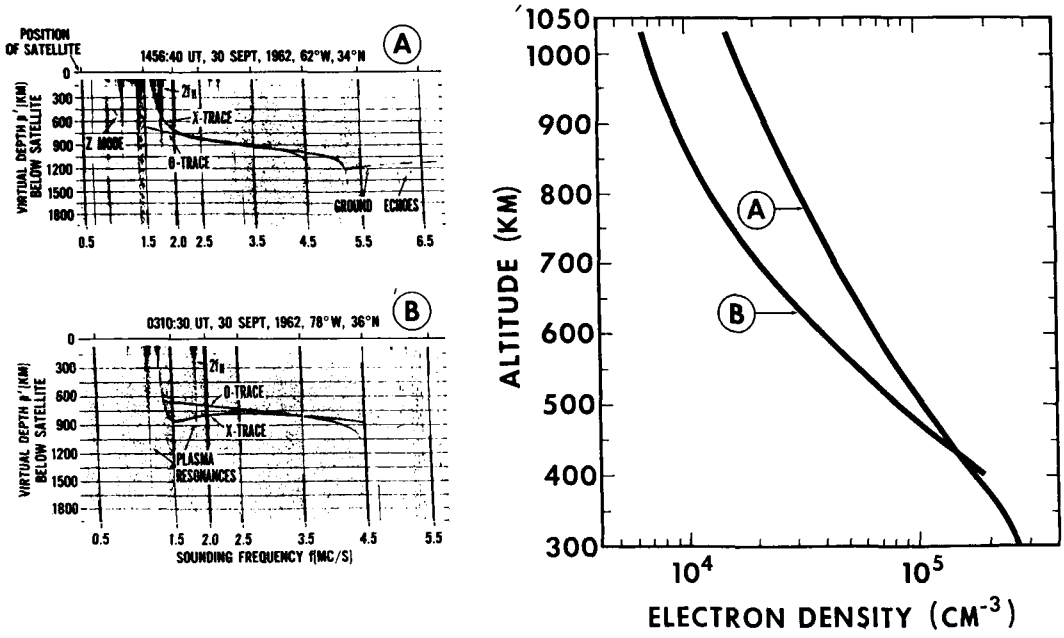

Fig. 1. Typical middle-latitude ionograms and corresponding true height profiles.

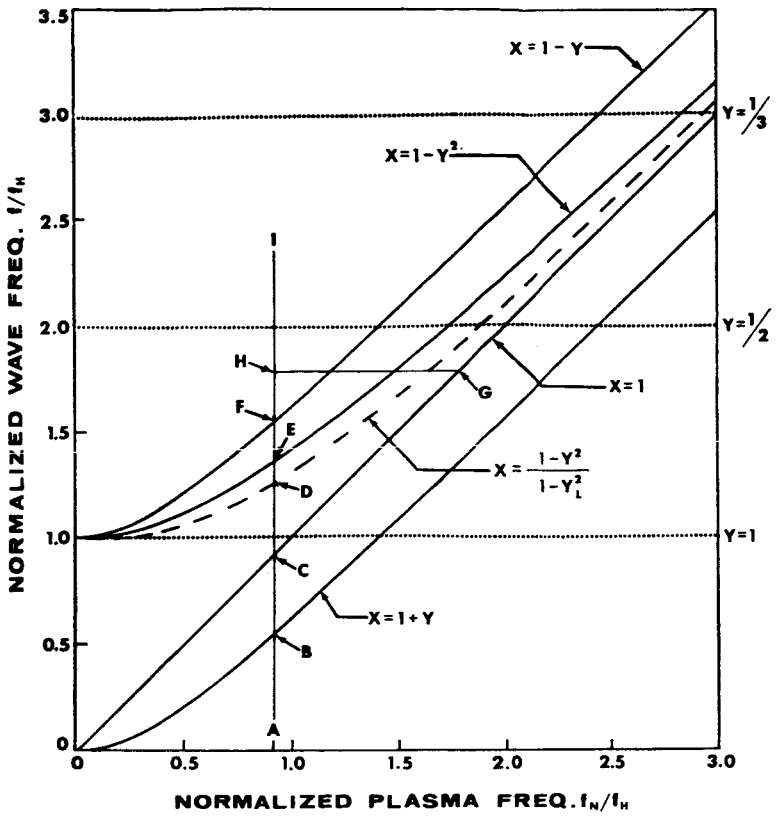

Fig. 2. Propagation and resonance conditions in a magnetoionic medium.

place until the point B on the curve $X = 1 + Y$ is reached, where propagation in the z mode can begin. This mode can propagate until $X = 1 - Y^2$ at point E, where z-mode propagation in any direction ceases. At point D, $X = (1 - Y^2)/(1 - Y_L^2)$ for the vertical ray (at 45° dip), the group retardation becomes very large as the energy propagates down to the reflection point $X = 1 + Y$ and returns. The process of propagating vertically to a reflection point and back can be represented by a horizontal line such as HG (for the ordinary ray) if we neglect the variation of gyrofrequency with altitude and further assume that plasma frequency increases in the direction of propagation. Propagation in the ordinary and extraordinary modes begins when $X \leqq 1$ and $X \leqq 1 - Y$ (points C and F), respectively.

The gyroresonances can occur when the sounder frequency is an integral multiple of the electron gyrofrequency, i.e., $Y = 1, 1/2, 1/3$, etc. Alouette observations of the gyrofrequency resonances, phenomena that are well known in plasma physics research [*Wharton*, 1959], have been qualitatively explained by *Lockwood* [1963]. The observed 'resonance' at $X = (1 - Y^2)/(1 - Y_L^2)$ for the vertical ray can be simply explained by the large group retardation encountered by the z mode as it propagates to the reflection point and returns.

Such a resonance and its fine structure are shown in Figure 3, which is a photograph of fifteen successive soundings separated by about 16 kc/s in wave frequency. This figure is a plot of signal amplitude (ordinate) as a function of time (abscissa) as the sounder sweeps from 1.202 to 1.451 Mc/s. One-millisecond timing marks enable the spectral components of this plasma resonance to be easily determined. The principal component of this resonance, 700 cps, does not change as the wave frequency increases 16 kc/s per pulse. The hydrogen ion gyrofrequency for this geomagnetic location is within 5 per cent of the measured principal spectral component. For this location (133.5°E, 16.5°S) and time (1623 UT, March 11, 1963), hydrogen is believed to be the predominant ion at the

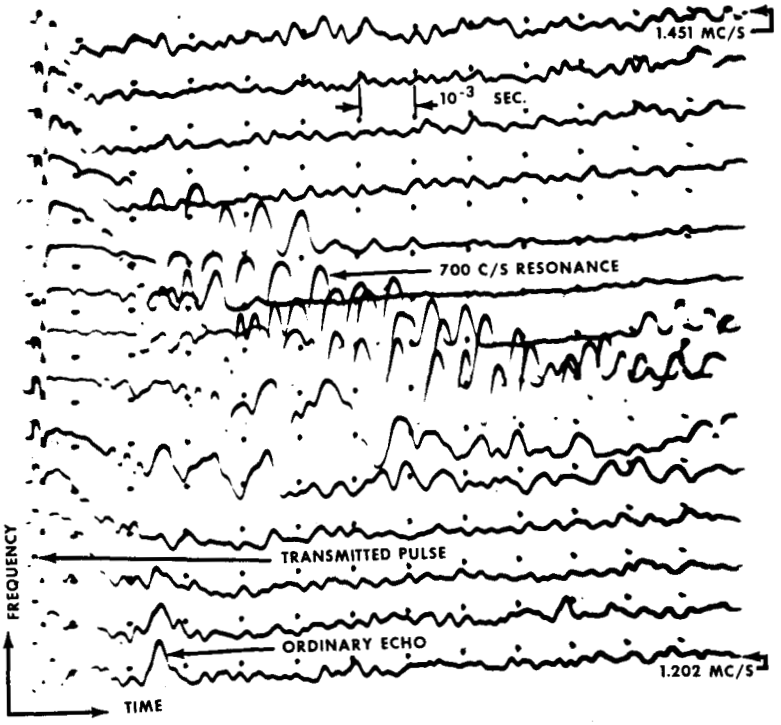

Fig. 3. Low-frequency oscillation observed in a plasma resonance.

satellite altitude [*Bauer*, 1962]. On the basis of these considerations, the observed periodicity may indeed be the hydrogen ion gyroresonance. This phenomenon is seen most frequently in geomagnetic locations where the magnitude of the field is largest, and on the conventional ionogram display it appears as a broken vertical line. The possibility that this oscillation is introduced by the satellite receiver is being investigated.

As can be seen from Figure 1, the z-mode trace does not appear on every ionogram, and the ordinary mode echoes usually are not seen at frequencies much lower than the extraordinary exit frequency ($X = 1 - Y$). J. W. King (private communication) has observed some ionograms near the magnetic equator on which the ordinary mode echoes extend back to the ordinary exit frequency, $X = 1$.

The echoes observed above 4.5 Mc/s (f_oF_2) on the ionogram shown in Figure 1*A* are returns from the ground; similar echoes have also been observed from sporadic E ionization on some ionograms. Spread F is observed from the topside and has been discussed by *Petrie* [1963] and *Knecht and Van Zandt* [1963]. As will be indicated later, oblique echoes have also been seen.

Reduction of p' — f records to $N(h)$ profiles. The initial step in the analysis of Alouette data is the conversion of sounding records to electron density distributions with altitude from which various ionospheric parameters can be inferred. The relation between the measured virtual depth of reflection p' from the satellite and the true depth of reflection p is

$$p' = \int_0^p \mu'(f, N, B, \theta)\, dp \qquad (1)$$

The group refractive index μ', given by the ratio of the free-space wave velocity to the group velocity, is a function of the wave frequency f, the electron density N, the magnitude of the magnetic field B, and the angle θ between the wave normal and the direction of B. For vertical propagation, θ is the complement of the magnetic dip angle. Although the group velocity V_g is a known function of electron density [*Shinn and Whale*, 1952], the determination of the depth p at which reflection occurs, i.e., the point at which $V_g = 0$, requires advance knowledge of

the electron density distribution $N(p)$. The heart of the $p' - f$ reduction problem therefore lies in the inversion of the integral in (1) that is necessary to determine p.

The problem must be approached by making assumptions about the electron density distribution, thereby approximating the $N(p)$ profile by a model. Various methods have been developed for the reduction of bottomside ionograms, and with appropriate modifications they can be applied to topside ionogram reduction. These methods fall roughly into two categories corresponding to the approximation made, viz., polynomial and lamination techniques. The polynomial technique developed independently by *Unz* [1961], *Titheridge* [1961], and *Knecht et al.* [1962] assumes that the entire profile can be approximated by a single polynomial in plasma frequency f_N. A modification of the single polynomial technique [*Titheridge*, 1961] approximates the profile by a number of overlapping polynomials. *Thomas et al.* [1963] have applied the single polynomial technique to topside reduction for the special case in which the geomagnetic field is neglected. The lamination method originally developed by *Budden* [1955] assumes that the profile can be approximated by a number of slabs or laminations, the height increments of which are a function of electron density. Budden assumed the height increments to be linear in plasma frequency, f_N (where $f_N = (8.98 \times 10^{-3})\sqrt{N}$ with f_N in megacycles per second and N in electrons per cubic centimeter); this technique has been used extensively by *Schmerling* [1957] and others. *Jackson* [1956] has developed a reduction method similar in principle with height increments linear in electron density. These lamination methods should properly be called first-order lamination methods, since the height increments are linear in plasma frequency or in electron density. Other lamination techniques developed by *Paul* [1960] and *Doupnik* [1963] assume height increments to be a parabolic function of electron density.

In applying a lamination method to the reduction of topside ionograms, it is logical to assume the height increments to be a function of the natural logarithm of electron density, log (N), since theoretical considerations [*Bauer*, 1962] and rocket experiments [*Jackson and Bauer*, 1961; *Bauer and Jackson*, 1962] indicate that the topside electron density distribution is essentially exponential in character. A similar exponential lamination technique has been proposed by *King* [1960] for the analysis of bottomside ionograms. The following sections outline the first-order linear-in-log (N) lamination method and its application to topside sounder ionogram reduction.

Exponential lamination method. Lamination methods of $p' - f$ reduction enable the integral in (1) to be approximated by a summation, i.e.,

$$p'_i = \int_0^{p_i} \mu'(f_i, N, B, \theta)\, dp \approx \sum_{j=1}^{i} \bar{\mu}'_{ij}(p_j - p_{j-1}) \qquad (2)$$

where p_i and p'_i are the true depth of reflection and virtual depth, respectively, for a wave with frequency f_i reflected at an electron density N_i, and $p_o = p'_o = 0$. $\bar{\mu}'_{ij}$ is the group refractive index for the frequency f_i as the wave passes through the slab defined by the true depths p_{j-1} and p_j. For example, $\bar{\mu}'_{53}$ represents the average value of μ' in the third slab for the frequency which is reflected at the bottom of the fifth slab. The expression for $\bar{\mu}'_{ij}$ is

$$\bar{\mu}'_{ij} = \frac{1}{p_j - p_{j-1}} \int_{p_{j-1}}^{p_j} \mu'(f_i, N, B, \theta)\, dp \qquad (3)$$

The calculation of $\bar{\mu}'_{ij}$ depends on the electron density distribution assumed within the slab. The linear-in-log (N) technique described here assumes that $N(p)$ is a simple exponential within each slab, i.e.,

$$N = N_{j-1} \exp\,[k_j(p - p_{j-1})] \qquad (4)$$

where N_{j-1} is the electron density at p_{j-1}, the distance from the satellite to the top of the slab, and $(k_j)^{-1} = (p_j - p_{j-1})/[\log (N_j) - \log (N_{j-1})]$ is the assumed constant electron-ion scale height for the slab. Solving (4) for p, differentiating with respect to $\log(N)$, and substituting the result into (3) yields

$$\bar{\mu}'_{ij} = \frac{1}{\log (N_j/N_{j-1})} \cdot \int_{\log (N_{j-1})}^{\log (N_j)} \mu'(f_i, N, B, \theta)\, \frac{dN}{N} \qquad (5)$$

Application of the exponential lamination method. The principal difference between the

reduction of topside sounder ionograms and conventional bottomside ionograms is that in the topside region the plasma frequency is nonzero over the entire ray path. A further complication is that the magnitude of the geomagnetic field varies appreciably over the ray path. For reduction of the ordinary trace, the field variation can be ignored for a first-order solution, but for reduction of the extraordinary trace the magnetic field is a very important parameter.

The electron density at the satellite is obtained from

$$N_0 = (1.2404 \times 10^4) f_{o_v}^2 \qquad (6)$$

for the ordinary trace ($X = 1$) and

$$N_0 = (1.2404 \times 10^4)(f_{x_v}^2 - f_{x_v} f_{H_v}) \qquad (7)$$

for the extraordinary trace ($X = 1 - Y$). The terms f_{o_v} and f_{x_v} are the wave frequencies in megacycles per second for the ordinary and extraordinary modes, respectively, at which the virtual depth is zero, and f_{H_v} is the electron gyrofrequency at the vehicle. The local gyrofrequency can be obtained from an inverse cube extrapolation of the ground value, from gyrofrequency plasma resonances, or by means of a polynomial fit to the geomagnetic field.

Since ionograms do not in general show an ordinary trace for wave frequencies much less than that at which propagation in the extraordinary mode begins, the electron density at the satellite can therefore only be determined by (7).

To begin the calculation of the profile, we compute the average group refractive index $\bar{\mu}'_{11}$ from (5) for the first lamination which is bounded by the electron density N_0 at the satellite and the electron density N_1 corresponding to the frequency of the first point scaled from the given $p' - f$ record. From (2) for $i = 1$, the true depth is given by $p_1 = p'_1 \bar{\mu}'_{11}$. The true altitude h_1 is found by subtracting p_1 from the satellite altitude h_v. To calculate the point on the profile corresponding to the reflection of a wave frequency f_i, the contribution to the retardation of f_i in the last lamination before reflection, $\bar{\mu}'_{ii}(p_i - p_{i-1})$, is found by subtracting from p'_i the retardation due to that part of the porfile already determined; from this result and the average group refractive index for the last lamination, p_i and h_i are then found by the following two equations:

$$p_i = p_{i-1} + \frac{p'_i - \sum_{j=1}^{i-1} \bar{\mu}'_{ij}(p_j - p_{j-1})}{\bar{\mu}'_{ii}} \qquad (8)$$

$$h_i = h_v - p_i \qquad (9)$$

This process is continued until the entire profile is determined.

Magnetic field effects. Although the dip angle for a given geographic location is nearly constant within the altitude range of topside soundings, the variation of the electron gyrofrequency can be as much as 25 per cent over the range 250 to 1000 km. Therefore the accurate determination of true height profiles requires allowing for the altitude variation of the magnitude of the field in the calculation of the integrals in (5). This variation can be taken into account by evaluating f_H at the altitude corresponding to the bottom of each lamination and assuming it to be constant throughout the lamination. This value of f_H is used in computing μ' and, when the propagation is in the extraordinary mode, f_H is also required to compute the upper limit of the integral of μ' in (5). A slight complication arises in computing the retardation for the last lamination, since the altitude of reflection (and hence f_H) is not known initially. This difficulty is overcome in the following manner: The average group refractive index $\bar{\mu}'_{ii}$ is calculated using f_H evaluated at the altitude corresponding to the top of the layer, h_{i-1}, and from (8) and (9) a value for h_i is obtained. The value of $\bar{\mu}'_{ii}$ is then recomputed using f_H evaluated at this initial h_i, and a new value of h_i is determined. Continuing this iterative process will not improve the degree of accuracy appreciably because of the approximation that f_H is a constant throughout the slab. Doupnik (private communication) has shown that by using only the extraordinary virtual depth for each lamination it is possible to improve the approximation by calculating the field as a function of altitude within the lamination, since the slope of the electron density profile for each lamination is the only unknown.

In most cases, the field compensation scheme described above is sufficiently accurate, i.e. the uncertainties in the true height calculations due to the field dependence are less than the uncertainties inherent in the reduction method. It has been found, however, that at locations where the extraordinary exit frequency and the local electron gyrofrequency are such that the

field parameter $Y = f_H/f$ is greater than about 0.7, the uncertainty in the first few true heights of reflection below the satellite (+20 km) is greater than the combined uncertainty due to scaling, computational, and satellite position errors (±10 km). This uncertainty is due to the extreme sensitivity of the index μ' and of the electron density calculations to slight deviations in Y when Y approaches unity. As the sounding frequency increases, Y decreases, and the uncertainties in the remaining true height calculations due to the field dependence become small.

Reduction of the ordinary ray data is much simpler, since the electron density at the bottom of the lamination is known, and therefore the height variation of Y within the lamination can be included more accurately by an iterative procedure. For the ordinary ray, the Y dependence of $d\mu'/dY$ for $\mu' > 2$ is large for two ranges of Y, $1/8 \lesssim Y \lesssim 1/2$ and $Y > 2$. The range $Y > 2$ is not encountered with the current topside sounder, and $Y \cong 1/2$ is seldom encountered in the altitude range where $\bar{\mu}' > 2$. Including the height variation of Y within each lamination does, however, reduce the error in a true height profile (for which $Y = 1/2$ at the satellite) by nearly 3 km over the entire profile.

Comparison of lamination methods applied to topside ionograms. When applying a lamination method to ionogram reduction, the error introduced by the departure of the assumed from the actual electron density distribution within each lamination can be determined by the number of laminations required to define the profile accurately. A comparison of the three first-order lamination reduction techniques applied to the extraordinary traces of the same ionogram is shown in Figure 4. The solid curve is the profile obtained by the linear-in-log (N) technique, while a single dashed curve shows the profiles obtained by the linear-in-N and linear-in-f_N techniques, since these last two agree with each other to within 4 km. The maximum difference in altitude between the two curves is about 20 km. Sixteen laminations were used in all three techniques. Doubling the number of laminations in all three techniques yields profiles which are identical (within 3 km) to the profile represented by the solid curve. Therefore, to calculate profiles of the same accuracy, fewer laminations are required by the linear-in-log (N) technique

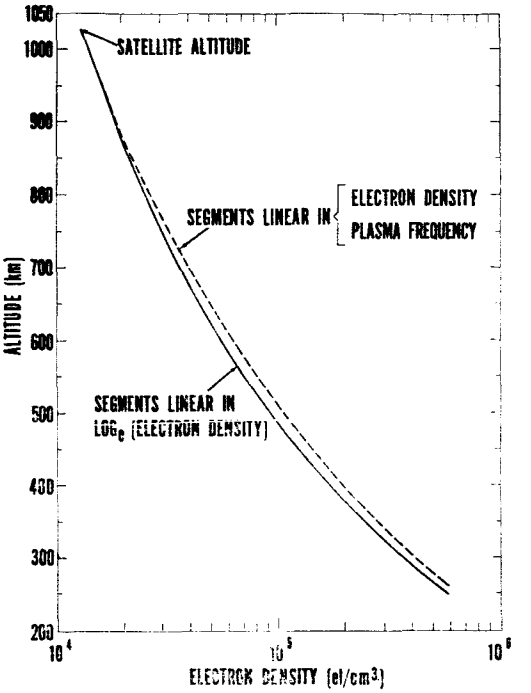

Fig. 4. Comparison of first-order lamination methods as applied to topside ionogram reduction.

than by the linear-in-N or linear-in-f_N techniques. If a height variation of higher order in log (N) were assumed, it is expected that even fewer laminations would be required.

$N(h)$ profiles. All methods of reducing ionograms to $N - h$ profiles assume that the wave normal is in the vertical direction. There is, however, evidence on some ionograms of field-aligned propagation. *Muldrew* [1963*b*] has discussed observations of trapping in field-aligned ducts near the magnetic equator. Figure 5 is an observed topside ionogram and two electron density distributions derived therefrom. Profile A, obtained on the assumption that the propagation path was entirely vertical, is obviously in error because it yields an F_2 maximum of 10^5 el/cm^3 at 100 km. Profile B, obtained on the assumption of field-aligned propagation, results in an F_2 maximum at 251 km. Although there is no direct evidence on this ionogram that the propagation is field aligned, this conclusion, based on the height of the F_2 maximum, is the only reasonable estimate of the actual conditions. It should be emphasized again that the over-all error in any data point due to scaling, computations, etc., is less than 10 km.

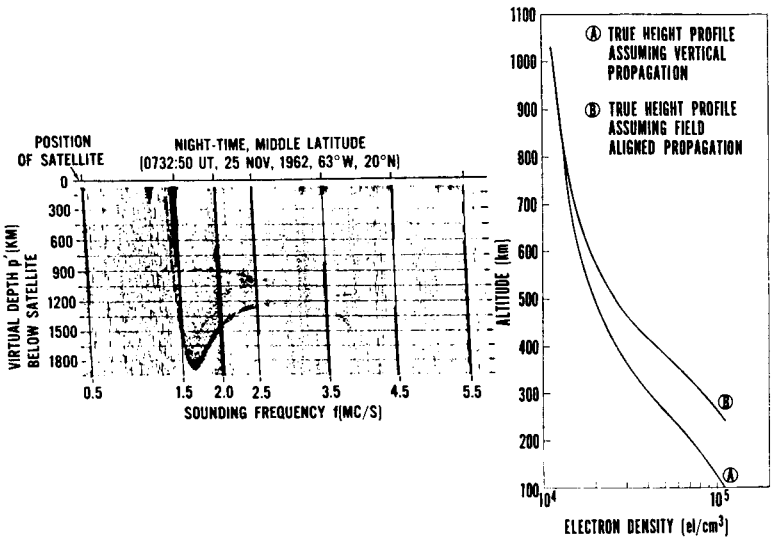

Fig. 5. One example of appreciable deviation from vertical propagation.

It is well known that a cusp will appear on a virtual height record whenever the slope of the electron density distribution is large and rapidly changing. The depth of this cusp depends principally on the slope, and the shape is a measure of the rate of change of the slope. The large cusp in Figure 5 at 1.65 Mc/s is produced by the change in scale height between 600 and 800 km. This cusp does not arise from the large values of the group refractive index that occur at $Y = 1$, since the largest value of Y for this sounding is 0.7. If the electron density distribution and electron gyrofrequency were such that $0.9 < Y < 1.0$, a sharp cusp would be observed in the extraordinary trace due to the variation of Y; however, this phenomenon has not yet been observed, since the electron densities observed at 1000 km are generally greater than 10^3 el/cm^3.

Summary and conclusion. Topside ionograms exhibit local phenomena (plasma resonances), echoes from the topside ionosphere (ordinary, extraordinary, and z propagation modes), and echoes from below the F_2 maximum (ground returns and sporadic E reflections). The range of extraordinary echoes extends rather consistently from the immediate vicinity of the satellite to the reflection point, and it is thus the most useful for calculating electron density profiles. Lamination methods of reducing $p' - f$ records to N–h profiles have been discussed and, in particular, a method using logarithmic laminations has been developed and applied to the topside ionosphere. This method yields greater accuracy than other first-order lamination techniques for a small number of sample points. The height variation of the geomagnetic field is important in (1) the computation of the average group refractive index in each lamination and (2) the calculation of the electron density at the boundaries of each lamination in the case of the extraordinary ray.

A convenient means of identifying the plasma resonances observed with a swept frequency topside sounder has been presented. In one of the plasma resonances a spectral component has been observed that appears to correspond to the H^+ gyrofrequency.

Some topside ionograms, reduced under the assumption of vertical propagation, yield profiles with a value of the F_2 peak that is obviously too low. It is suggested that in these cases field-aligned propagation is the source of this error.

Acknowledgments. The continuous operation of the swept frequency topside sounder satellite launched more than a year ago is a tribute itself to the excellent work of the Defence Research Telecommunications Establishment. Many helpful discussions with J. E. Jackson and S. J. Bauer of the Goddard Space Flight Center are hereby acknowledged. We are indebted to J. Doupnik for the group refraction index computer subroutine,

whose accuracy was verified by comparing with *Becker's* [1960] values.

References

Bauer, S. J., On the structure of the topside ionosphere, *J. Atmospheric Sci., 19,* 276, 1962.

Bauer, S. J., and J. E. Jackson, Rocket measurement of the electron density distribution in the topside ionosphere, *J. Geophys. Res., 67,* 1675, 1962.

Becker, W., Tables of ordinary and extraordinary refractive indices, group refractive indices and $h_{o,x}'(f)$-curves for standard ionospheric layer models, *Max-Planck Inst. Aeronomy,* no. 4, 1960.

Budden, K. G., *Cambridge Conference on Ionospheric Physics,* p. 332, Physical Society, London, 1955.

Doupnik, J. R., A flexible method of determining the electron density in the ionosphere, *Penna. State Univ. Sci. Rept. 190,* 1963.

Hagg, E. L., A preliminary study of the electron density at 1000 kilometers, *Can. J. Phys., 41,* 195–199, 1963.

Jackson, J. E., A new method for obtaining electron-density profiles from p'-f records, *J. Geophys. Res., 61,* 107, 1956.

Jackson, J. E., and S. J. Bauer, Rocket measurements of a daytime electron density profile up to 620 kilometers, *J. Geophys. Res., 66,* 3055, 1961.

King, G. A. M., Use of logarithmic frequency spacing in ionogram analysis, *J. Res. NBS, 64D,* 501, 1960.

Knecht, R. W., and T. E. Van Zandt, Some early results from the ionospheric topside sounder satellite, *Nature, 197,* 641, 1963.

Knecht, R. W., T. E. Van Zandt, and J. M. Watts, Electron density profiles in the ionosphere and exosphere, *NATO Conf. Ser., 2,* 246, 1962.

Lockwood, G. E. K., Plasma and cyclotron spike phenomena observed in topside ionograms, *Can. J. Phys., 41,* 190–194, 1963.

Muldrew, D. B., The relationship of F-layer critical frequencies to the intensity of the outer Van Allen belt, *Can. J. Phys., 41,* 199–202, 1963*a*.

Muldrew, D. B., Radio propagation along magnetic field-aligned sheets of ionization observed by the Alouette topside sounder, *J. Geophys. Res., 68,* 5355–5370, 1963*b*.

Nelms, G. L., Scale heights of the upper ionosphere from topside soundings, *Can. J. Phys., 41,* 202–206, 1963.

Paul. A. K., Aktive Hochfrequenzspektrometer für Ionosphärische Echolotung, *A.E.U., 14,* 468, 1960.

Petrie, L. E., Topside spread echoes, *Can. J. Phys., 41,* 194–195, 1963.

Ratcliffe, J. A., *The Magnetoionic Theory and its Applications to the Ionosphere,* Cambridge University Press, London, 1959.

Schmerling, E. R., The reduction of h'-f records to electron-density-height profiles, *Penna. State Univ. Sci. Rept. 94,* 1957.

Shinn, D. H., and H. A. Whale, Group velocities and group heights from the magnetoionic theory, *J. Atmospheric Terrest. Phys., 2,* 85, 1952.

Thomas, J. O., A. R. Long, and D. Westover, The calculation of electron density profiles from topside sounder records, *J. Geophys. Res., 68,* 3237, 1963.

Titheridge, J. E., A new method for the analysis of ionospheric $h'(f)$ records, *J. Atmospheric Terrest. Phys., 21,* 1, 1961.

Unz, H. A., A solution of the integral equation $h'(f) = \int \mu' (f, f_0) dz(f_0)$, *J. Atmospheric Terrest. Phys., 21,* 40, 1961.

Warren, E. S., Sweep-frequency radio soundings of the topside of the ionosphere, *Can. J. Phys., 40,* 1692, 1962.

Wharton, C., *Proc. 4th Intern. Conf. Ionization Phenomena on Gases,* North-Holland Publishing Co., Amsterdam, 1959.

Calvert, W., and G. B. Goe, Plasma resonances in the upper atmosphere, submitted to *J. Geophys. Res.,* 1964.

(Manuscript received October 30, 1963.)